Oceanic influences for a large eye of Typhoon Talas in 2011

Akiyoshi Wada*

*Meteorological Research Institute, Tsukuba, Ibaraki, 305-0052, JAPAN

awada@mri-jma.go.jp

1. Introduction

Tropical cyclones with a large eye are often called as 'annular' tropical cyclones, a symmetric category of tropical cyclones (Knaff et al., 2003). According to Weatherford (1984), eyes with diameters > 85 km are considered to be large. The radius of 15 kt wind speed of Typhoon Talas was from 500 to 650 km when its minimum central pressure was 970 hPa. Talas made landfall in Japan at around 1000 JST on 3 September and caused torrential rainfalls particularly the Kii peninsula. One of peculiar features of Talas was the maintenance of a large eye when Talas moved northward and turned to northwestward until the typhoon made landfall in Japan. The translation speed of Talas was estimated to be nearly 1.3 m s^{-1} from 26 to 30 August, which was slower than the phase speed of the first baroclinic mode in the ocean. The slow translation speed of Talas is considered to be favorable for lowering sea surface temperature beneath the typhoon.

In order to understand oceanic influences on Talas, particularly its large eye, numerical simulations were performed using a nonhydrostatic atmosphere model coupled with an ocean wave model and a multi-layer ocean model (Wada et al., 2010). The surface roughness length calculated by the coupled model is derived from the formulation based on wave steepness (Taylor and Yelland, 2001).

2. Experimental design

Summary of numerical simulations performed by the atmosphere-wave-ocean coupled model is listed in Table 1. The coupled model covered nearly a 3600 km x 5000 km computational domain with a horizontal grid spacing of 6 km. The coupled model had 40 vertical levels with variable intervals from 40 m for the near-surface layer to 1180 m for the uppermost layer. The coupled model had maximum height approaching nearly 23 km. The integration time was 120 hours (120 h) with a time step of 15 s in the coupled model. The time step of the ocean model is six times that of the coupled model.

Table 1 Summary of ocean coupling/noncoupling, parameters of Rayleigh damping associated with the lateral boundary condition (PRD), and horizontal resolution of MOVE reanalysis of the coupled model.

Experiment	Ocean coupling	PRD	Horizontal resolution of MOVE reanalysis
A1 IDIFX15	NO	15	0.1º
C1_IDIFX15	YES	15	0.1º
A5_IDIFX15	NO	15	0.5º
C5_IDIFX15	YES	15	0.5º
C5_IDIFX5	YES	5	0.5º
C5_IDIF150	YES	150	0.5º

The sensitivity of parameters (the value of horizontal grids is 5, 15, 150, respectively) of Rayleigh damping associated with the lateral boundary condition to the simulated track of Talas was investigated in order to examine the influence of environmental atmospheric conditions on the track of Talas.

Oceanic initial conditions were obtained from the oceanic reanalysis datasets with horizontal resolutions of 0.1º and 0.5º calculated by the Meteorological Research Institute multivariate ocean variational estimation (MOVE) system (Usui, et al., 2006). Because the southern limit of the domain in the MOVE system with a horizontal resolution of 0.1º was 15ºN, the oceanic reanalysis data with a horizontal resolution of 0.5º were merged south of 15ºN when the oceanic reanalysis data with a horizontal resolution of 0.1º was used as an oceanic initial condition.

3. Results

Figures 1a-b show the results of track simulations and the best track of Talas. Simulated Talas moved north along 139˚E from 12 h to 54 h in A5_IDIFX15 (Table 1), whereas the best track of Talas indicates the northward translation along 140˚E and then turn to northwestward from 0600 UTC 30 August (at 90 h). The parameters of Rayleigh damping associated with the lateral boundary condition clearly affected the track of Talas: When the value was high, simulated Talas tended to move westward, while the typhoon tended to move northward when the value was low (Fig. 1a).

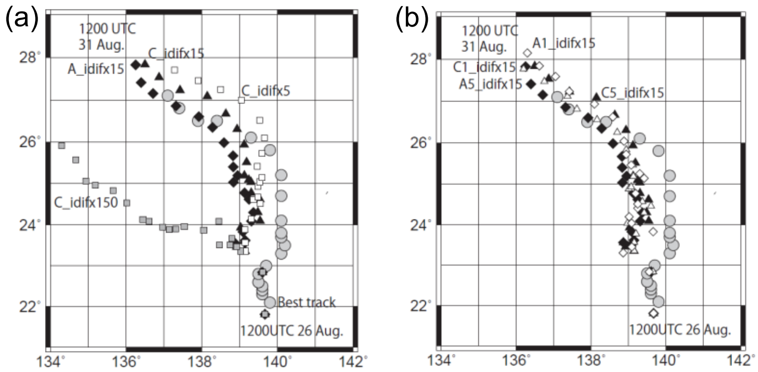

Figure 1 (a) Best track and simulated tracks in A5_IDIFX15 (close diamonds), C5_IDIFX15(close triangles), C5_IDIFX5(open squares), and C5_IDIFX150(gray squares). (b) Same as Fig.1(a) except in A5_IDIFX15, C5_IDIFX15, A1_IDIFX15 (open diamonds), and C1_IDIFX15 (open triangles).

A difference of initial oceanic condition led to a difference of the time when the simulated Talas was recurved: When the oceanic reanalysis data with a horizontal resolution of 0.5° were used, the recurvature occurred earlier (54 h in A5_IDIFX15 and 60 h in C5_IDIFX15) than that (72 h in A1_IDIFX15 and 78 h in C1_IDIFX15)when the data with a horizontal resolution of 0.5° were used (Fig.1b).

Figure 2 show the time series of simulated central pressures and best-track central pressure when the parameter of Rayleigh damping associated with the lateral boundary condition was set to 15. Simulated central pressures in A1_IDIFX15 and A5_IDIFX15 underwent rapid intensification from 24 h to 60 h, corresponding to the northward translation of Talas. A central pressure minimum in A1_IDIFX15 was 938.2 hPa in A1_IDIFX15 (at 96 h) and 942.6 hPa in A5_IDIFX (at 120 h), while a central pressure minimum was 968.9 hPa in C5_IDIFX15 (at 60 h) and 966.5 hPa in C1_IDIFX15 (at 72 h). The central pressure minima in C1_IDIFX15 and C5_IDIFX15 were closer to the best-track central pressure minimum (970hPa) than those in A5_IDIFX15 and A1_IDIFX15.

As described in the introduction, a large eye of Talas is one of peculiar features in that a large eye had no debris or mesovortex inside the eyewall, differently from previous annular hurricanes (Knaff et al., 2003) and Typhoon Winnie in 1997 (Zhang et al., 2005). Figure 3 indicates the time series of the radius of maximum wind speed at the lowermost level (corresponding to the height of 20 m). After 48 h, the radius seems to be stationary and become large monotonically. The average of the radius from 48 h to 120 h was 94.7 km in A5_IDIFX, 92.0 km in A1_IDIFX, 108.3 km in C5_IDIFX and 103.5 km in C1_IDIFX, indicating that the ocean coupling results in the enlargement of the radius of maximum wind speed of Talas.

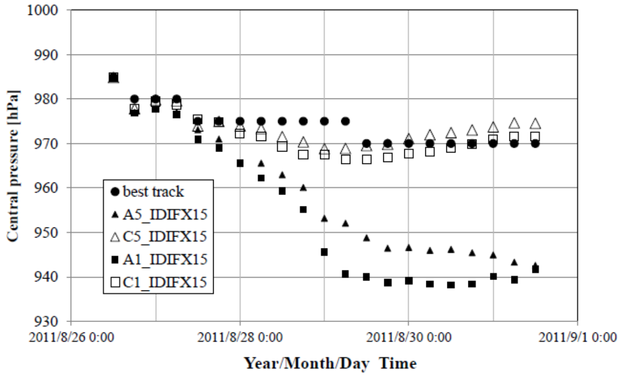

Figure 2 Time series of central pressures in A5_IDIFX15, C5_IDIFX15, A1_IDIFX15 and C1_IDIFX15.

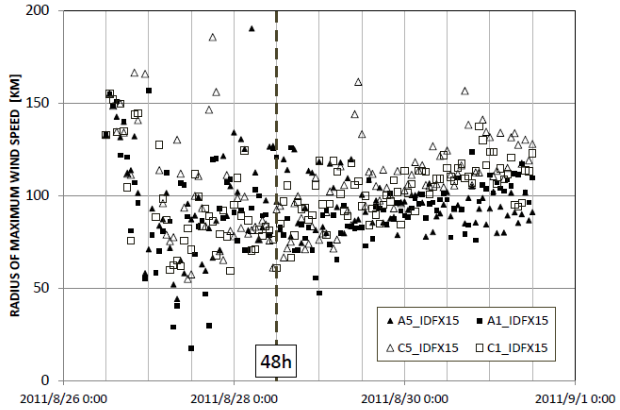

Figure 3 Same as Fig. 2 except for the radius of maximum wind speed at the lowermost level of the coupled model.

4. Discussion and conclusion

The results of the numerical simulations suggest that the upper ocean response (including sea-surface cooling beneath the typhoon) to Talas contributes to the enlargement of the radius of maximum wind speed of Talas to some extent in addition to the suppression of its excessive intensification. The sensitivity experiments associated with the parameters of Rayleigh damping suggests that excessively high value interrupts the precise track simulation of Talas. However, Talas was indeed formed in the eastern part of the subtropical cyclonic gyre and the gyre included Typhoon Nanmadol in the western part of the gyre. How the gyre affected Talas directly or indirectly as an atmospheric environmental factor should be explored because it is considered to be related to how much the value of Rayleigh damping parameter should be set.

For Talas, the horizontal resolution of 6 km is sufficient to reproduce the (maximum) intensity of Talas. For a typhoon with a large eye, ocean coupling might be indispensable for reproducing the intensity realistically.

Acknowledgement

This work was supported by the Japan Society for the Promotion of Science (JSPS), Grant-in-Aid for Scientific Research (C) (22540454) and on Innovative Areas (Research in a proposed research area) (23106505).

References

Knaff, J. A., J. P. Kossin, and M. DeMaria (2003), Annular hurricanes. *Wea. Forecasting*, **18**, 204-223.

Taylor, P. K., and M. J. Yelland (2001), The dependence of sea surface roughness on the height and steepness of the waves. *J. Phys. Oceanogr.*, **31**, 572-590.

Usui, N., S. Ishizaki, Y. Fujii, H. Tsujino, T. Yasuda, and M. Kamachi (2006), Meteorological Research Institute multivariate ocean variational estimation (MOVE) system: Some early results. *Advances in Space Research*, **37**, 896-822.

Wada, A., N. Kohno and Y. Kawai (2010), Impact of wave-ocean interaction on Typhoon Hai-Tang in 2005, *SOLA*, **6A**, 13-16.

Weatherfold, C. L. (1984), Typhoon structural variability. Colorado State University, Atmospheric Science Paper 391, 77pp.

Zhang, Q.-H., Chen, S.-J., Kuo, Y.-H., Lau, K.-H., and R. A. Anthes (2005), Numerical study of a typhoon with a large eye: Model simulation and verification. *Mon. Wea. Rev.*, **133**, 725-742.